Materials Science Forum
ISSN: 1662-9752, Vol. 925, pp 90-97
doi:10.4028/www.scientific.net/MSF.925.90

Submitted: 2017-11-29
Revised: 2017-12-14
Accepted: 2018-01-10
Online: 2018-06-20

On the Primary Solidification of Compacted Graphite Iron: Microstructure Evolution during Isothermal Coarsening

Juan Carlos Hernando[1,a*], Attila Diószegi[1,b]

[1]Department of Materials and Manufacturing, Jönköping University, Gjuterigatan 5, SE 551 11, Jönköping, Sweden

[a]Juan-Carlos.Hernando@ju.se, [b]Attila.Dioszegi@ju.se

Keywords: Primary austenite, Microstructure evolution, Dendritic coarsening, Compacted Graphite Iron, CGI

Abstract It is widely accepted that in most commercial hypoeutectic alloys, both static mechanical properties and feeding characteristics during solidification, are extremely linked to the coarseness of the primary phase. It is therefore of critical importance to provide tools to control and predict the coarsening process of the dendritic phase present in hypoeutectic melts. The characterization of the primary phase, a product of the primary solidification, has traditionally been neglected when compared to the eutectic solidification characterization in cast iron investigations. This work presents the morphological evolution of the primary austenite present in a hypoeutectic compacted graphite cast iron (CGI) under isothermal conditions. To that purpose, a base spheroidal graphite cast iron (SGI) material with high Mg content is re-melted in a controlled atmosphere and reversed into a CGI melt by controlling the Mg fading. An experimental isothermal profile is applied to the solidification process of the experimental alloy to promote an isothermal coarsening process of the primary austenite dendrite network during solid and liquid coexistence. Through interrupted solidification experiments, the primary austenite is preserved and observed at room temperature. By application of stereological relations, the primary phase and its isothermal coarsening process are characterized as a function of the coarsening time applied. The microstructural evolution observed in the primary austenite in CGI and the measured morphological parameters show a similar trend to that observed for lamellar graphite cast iron (LGI) in previous investigations. The modulus of the primary austenite, Mγ, and the nearest distance between the centre of gravity of neighbouring austenite particles, Dγ, followed a linear relation with the cube root of coarsening time.

Introduction

In the last decades, compacted graphite cast iron, CGI, has become a popular material for numerous automotive applications due to its excellent properties [1]. The good combination of thermal and mechanical properties makes CGI an ideal candidate material for designers and engineers working, for instance, with engine blocks and cylinder heads in the heavy truck industry, which are simultaneously subjected to mechanical and thermal loads [2]. The final properties of CGI, as a cast material, are related to the microstructure formed during the solidification process. In the case of the hypoeutectic Fe-C alloys (CE<4.35), the solidification starts with the formation of the primary phase to later continue with the nucleation and growth of the graphite. The intermediate response in terms of thermal properties of CGI when compared to SGI and lamellar graphite cast iron (LGI), is associated to the intermediate character of the vermicular graphite shape, characteristic of CGI [3]. The mechanical properties in hypoeutectic Fe-C alloys have been found to be influenced in a major manner by the fraction and the final morphology of the primary dendrites, which have been reported to be related to the UTS in recent LGI investigations [4]. At the same time, the size of eutectic cells in LGI has been found to be dependent on the morphological size-scale of the primary austenite and its coarseness [5], presenting an important relationship between the eutectic solidification and the morphology of the final structure obtained during the primary solidification in hypoeutectic cast irons.

The final morphology of the primary structure, consisting on the primary dendrites formed during the primary solidification, is governed by a coarsening process [6] which minimizes the interfacial free energy of the system by decreasing the interfacial area per volume [7]. Throughout this diffusional process, the length scale of the system increases, and the total interfacial area decreases [8]. The understanding of the coarsening process and any related morphological changes in the dendritic structures of cast iron alloys during solidification is of technological importance to predict and tailor the final component properties and design a correct interdendritic feeding during solidification [9]. In cast alloys, the existence of complex structures such as dendrites, promoted that the microstructural coarsening process of primary structures has been traditionally studied in terms of the secondary dendrite arm spacing (SDAS) [10], which follows a linear relation with the cube root of the time over which solid and liquid coexist, $t^{1/3}$ [11]. Nevertheless, the severe morphological changes induced by the coarsening process after long coarsening times [12] leading to dendrite fragmentation [13] and further coalescence [14] made necessary the use of shape-independent size scales to describe the complete microstructural evolution [15]. A new set of shape-independent parameters based on stereological relations have been used in some recent works studying the dynamic [16] and the isothermal coarsening process [14] of primary austenite in lamellar graphitic irons. The use of these stereological parameters, the modulus of primary austenite, M_γ, the distance between austenite particles, D_γ, and the hydraulic diameter of the interdendritic phase, D_{IP}^{hyd}, allowed the quantitative characterization of the complete isothermal coarsening process of primary austenite, showing that both in dynamic and isothermal coarsening these parameters follow a linear relation to the cubic root of coarsening time, $t^{1/3}$ [14, 16].

Despite the increasing industrial interest on CGI, there is still a critical issue related to the control of nucleation and growth mechanisms of graphite [9] that hindered the study of the solidification of CGI under laboratory conditions for many years. The recent development of a new experimental technique to produce graphitic irons with controlled nodularity after a re-melting process [17] and an experimental procedure applied to study the isothermal coarsening of lamellar graphitic cast iron [18] enables the possibility to study the isothermal coarsening of the primary austenite in CGI. The scope of this work is to study the morphological evolution of primary austenite in CGI under isothermal conditions applying both experimental techniques mentioned above. The morphological parameters used in previous works in lamellar graphitic cast iron investigations, are applied to characterize the isothermal evolution of primary austenite in compacted graphitic cast iron and to the comparison of the coarsening rate of primary austenite in LGI and CGI.

Experimental Procedure

The base SGI alloy was cast in a furan sand mould with 25 cylindrical cavities of 50 mm diameter and 300 mm in height. FeSiMg was used for the nodularization treatment using the tundish ladle method, while inoculation was added during the pouring process. The chemical composition of the base SGI, shown in Table 1, was determined by optical emission spectrometry (OES) of a quenched coin produced immediately before the pouring process. Cylindrical specimens of 38 mm diameter with a weight of 400 ± 0.5 g and an approximate height of 42 mm were produced from the base SGI cylinders.

Table 1: Chemical composition of the base SGI alloy. CE = C + 1/3 (Si + P).

Element	C	Si	Mn	P	S	Cu	Sn	Mg	CE
Weight percent	3.4	2.5	0.68	0.030	0.010	0.87	0.11	0.063	4.2

The experimental equipment is formed by a resistance furnace where a cylindrical specimen of the base SGI is re-melted and re-solidified after a certain holding time resulting in specimens of dimensions Ø40 x 40 mm [16]. The re-melting process consists of a thermal cycle of 75 min from room temperature to 1723 K (1450 °C) followed by a holding time and a solidification process. The whole process is performed under the neutral atmosphere provided by an argon flow. The holding

time is adjusted to control the fading process of Mg in the base SGI in order to produce a final CGI material with the desired nodularity [17]. Based on previous investigations, the holding time to produce a CGI material with a nodularity lower than 5% with the current experimental setup, is calculated to be 80 min. Two type-S thermocouples are placed at the middle section of the specimen, providing thermal data of the solidification process and allowing the estimation of the thermal coherency temperature [18]. The solidification process following the re-melting and holding time is halted after this thermal coherency point when a coherent dendritic primary austenite structure has been formed. Then an isothermal treatment at 1436 K (1163 °C) is applied promoting an isothermal coarsening process of the primary austenite microstructure. After the end of the isothermal treatment, the sample is quenched into agitated water, preserving the primary dendritic microstructure and promoting a metastable eutectic solidification for the remaining liquid. Samples are coarsened for 10, 30, 60 and 90 min. An additional sample for 0 min of isothermal treatment is produced by quenching from the thermal coherency temperature to observe the original coherent dendritic microstructure preceding the isothermal treatment. An extra series of experiments is conducted to evaluate the possible influence of the isothermal treatment in the fading process of Mg and thus in the final nodularity of the specimen. In this series of experiments, the furnace is turned-off after the isothermal treatment, starting a new cooling process that re-starts the solidification process of the sample, which is cooled to room temperature inside the furnace. Samples are isothermally coarsened for 0, 10, 30, 60 and 90 min, then after the isothermal treatment, the solidification is re-started.

All the samples produced in both experimental series of this work, the quenching series and the re-started solidification series, are sectioned perpendicularly to the longitudinal axis approximately at its middle section, around 20 mm from the bottom end. Then the samples are mounted in thermosetting resin, ground with SiC papers of different granulometries and polished with suspensions containing diamond particles of 3 and 1 μm. The quenched samples are then etched after the polishing process by application of a new etching technique for cast iron quenched samples consisting of additional polishing steps of 20 seconds with the 1 μm diamond suspension, which make the austenite dendrites clearly distinguishable [19] as can be seen in Fig. 1 a). A Wacom Cintiq interactive pen display combined with an automatic colour selection technique is applied to transform the etched micrographs from the quenched samples micrographs into binary images where dendrites are represented as black colour entities, as shown in Fig. 1 b).

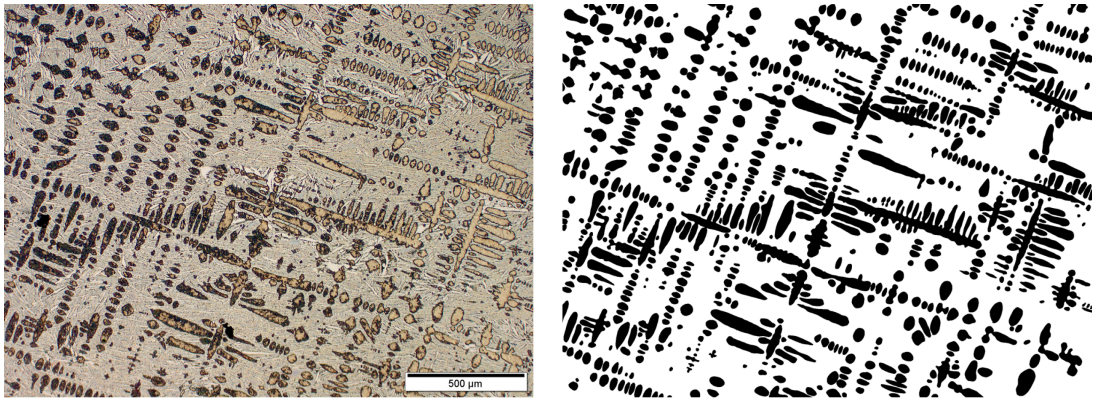

a) b)

Figure 1: a) Representative micrograph of the quenched sample after an isothermal treatment of 0 min, b) binary image of the same micrograph prepared for quantitative analysis.

The quantitative analysis of the microstructure from the quenched samples is performed by measuring relevant microstructural parameters on the binary images. The fraction of primary austenite, f'_γ, Eq.1, the modulus of primary austenite, M'_γ [μm], Eq.2, the hydraulic diameter of the interdendritic phase, D_{IP}^{Hyd} [μm], Eq.3, and the spatial distribution of the austenite particles, D_γ, which measures the smallest distance between the centre of gravity of one austenite particle and the centres of gravity of its surrounding neighbours, are selected for their use in the characterization of

coarsening phenomena in recent cast iron literature and therefore to facilitate a comparison between the results obtained in the current work on CGI and the published literature on coarsening of LGI [14, 16, 18, 19]. The quantitative measurements are done with the Olympus Stream Motion Desktop software 1.9.1.

$$f'_{\gamma} = \frac{V_{\gamma'}}{V_T} = \frac{A_{\gamma'}}{A_T} \quad (1)$$

$$M'_{\gamma} = \frac{V_{\gamma'}}{S_{\gamma'}} = \frac{A_{\gamma'}}{P_{\gamma'}} \quad (2)$$

$$D_{IP}^{Hyd} = \frac{V_{IP}}{S_{IP}} = \frac{A_{IP}}{P_{IP}} = \frac{A - A_{\gamma'}}{P_{\gamma'}} \quad (3)$$

Where the variables V, A, S and P represent: volume, area, interfacial surface area and perimeter, respectively. The subscripts: T, γ', and IP, refer to total, primary austenite, and interdendritic phase, respectively.

The nodularity of the samples produced in the re-started solidification series is characterized following the ISO 16112:2017 standard [20] after the polishing process, Fig. 2 a), using optical micrographs representing a minimum area of 30 mm^2 for each specimen. After the characterization of the nodularity and the measurement of the graphite fraction, the samples produced in the re-started solidification series, are colour-etched at 381 K (108 °C) for approximately 6 min with Motz's reagent [21], Fig. 2 b).

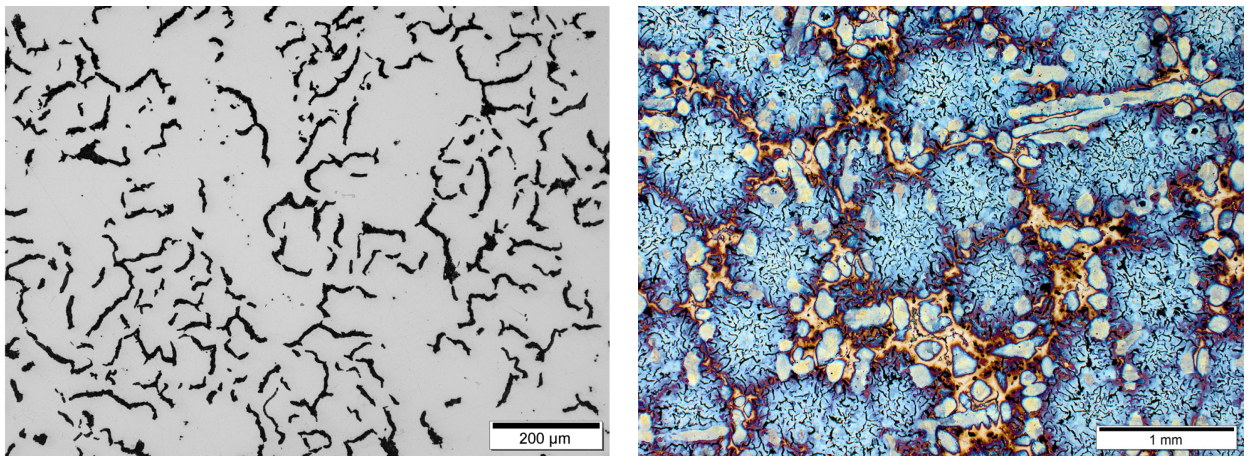

a) b)

Figure 2: a) Representative polished micrograph of a sample with re-started solidification after an isothermal treatment of 60 min, b) colour-etched micrograph of the same sample after Motz's reagent etching.

Results and Discussion

The quantitative analysis applied to the quenched samples shows that the measured local area fraction of primary austenite, f_{γ}, remains stable, around 31%, for all quenched samples independent of the coarsening time, Fig. 3 a). This result indicates that the isothermal treatment did not promote any nucleation and growth event and that the changes in the austenite morphology are due to a microstructural coarsening process.

The modulus of primary austenite, M_{γ}, describes the reduction of surface area to volume ratio of the austenite phase. In a two-dimensional investigation, it is expressed as the ratio between the area of a phase and its periphery of the phase. For the current investigation, M_{γ}, shows a stable linear relation to $t^{1/3}$ for all the samples as can be seen in Fig. 3 b). The spatial distribution of the microstructural coarsening process, characterized by the hydraulic diameter of the interdendritic phase (D_{IP}^{hyd}), shown in Fig. 3 c), and the distance to the nearest austenite particle (D_{γ}), Fig. 3 d), shows an increase with the coarsening time that can be observed in both parameters. This suggests that not only the

distance between the centre of gravity of austenite particles is increasing (D_γ) as a direct result of the reduction of surface area to volume ratio, but also the space between the austenite particles (D_{IP}^{hyd}). The comparison between the coarsening rate of the primary austenite in LGI and CGI, shows no significant alteration, exhibiting a very similar value. The difference in the numerical values in the measured parameters is attributed to a different initial growth event, related to the starting point of the isothermal treatment performed, which is associated to a small difference in the austenite fraction, linked to small chemical composition variations, between the two alloys compared in this work.

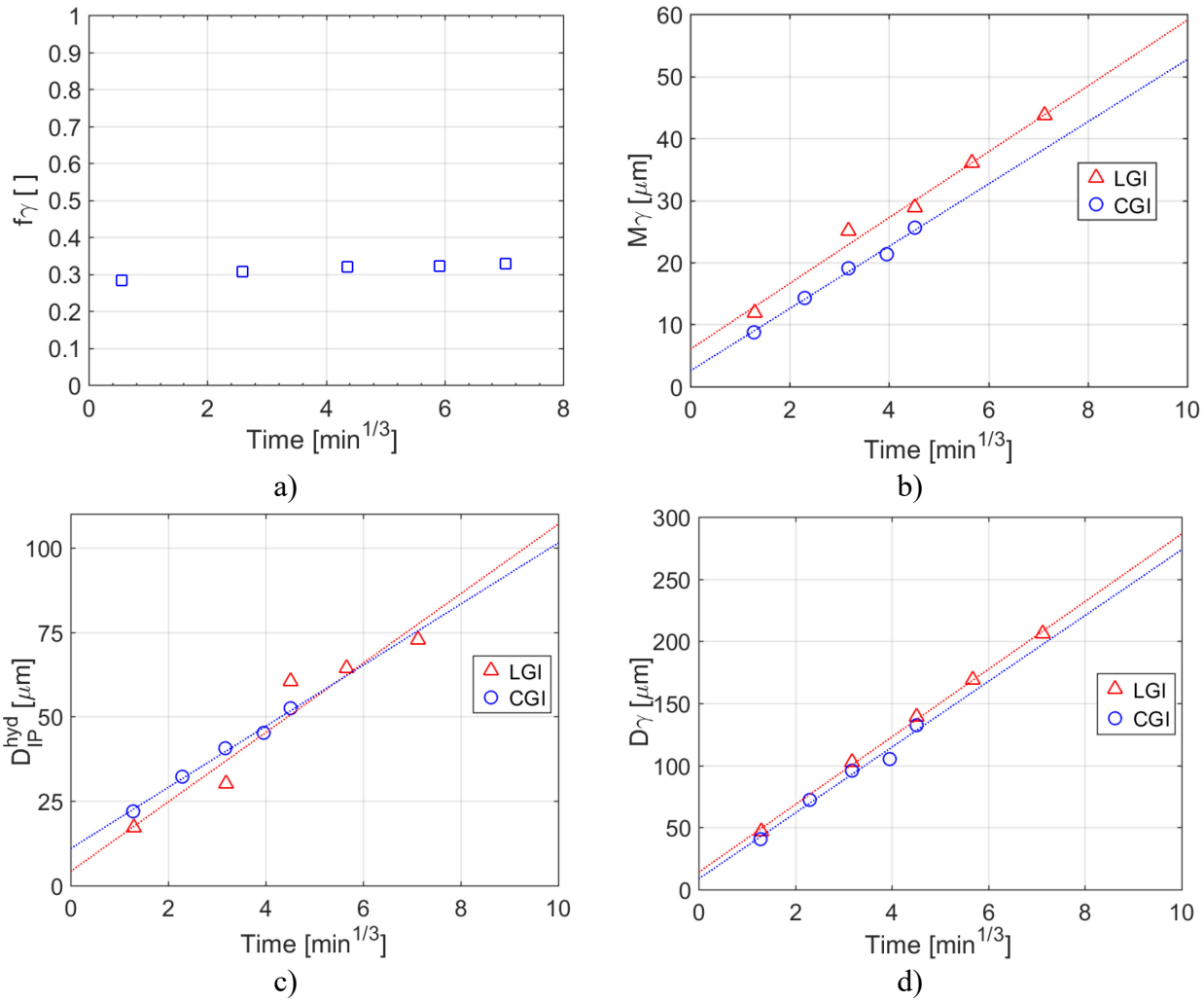

Figure 3: a) Measured area fraction of primary austenite, f_γ, b) modulus of the primary austenite phase, M_γ, c) hydraulic diameter of the interdendritic phase, D_{IP}^{hyd}, and d) distance between austenite particles, D_γ as a function of time. In the b), c) and d) figures, the circles represent the values from the current investigation, related to CGI material, while the triangles represent the literature data for a similar investigation performed in LGI [14].

The graphite fraction measured in the samples produced in the re-started solidification series, shows a stable mean value of 11%, Fig. 4 a), while the nodularity rests around 2% according to ISO standard for all the samples produced in the series, Fig. 4 b). These observations clearly reveal that these two parameters, of critical importance when characterizing the eutectic solidification of graphitic cast irons, remain constant for the whole series and show no dependence to the isothermal coarsening time applied in the liquid-solid region.

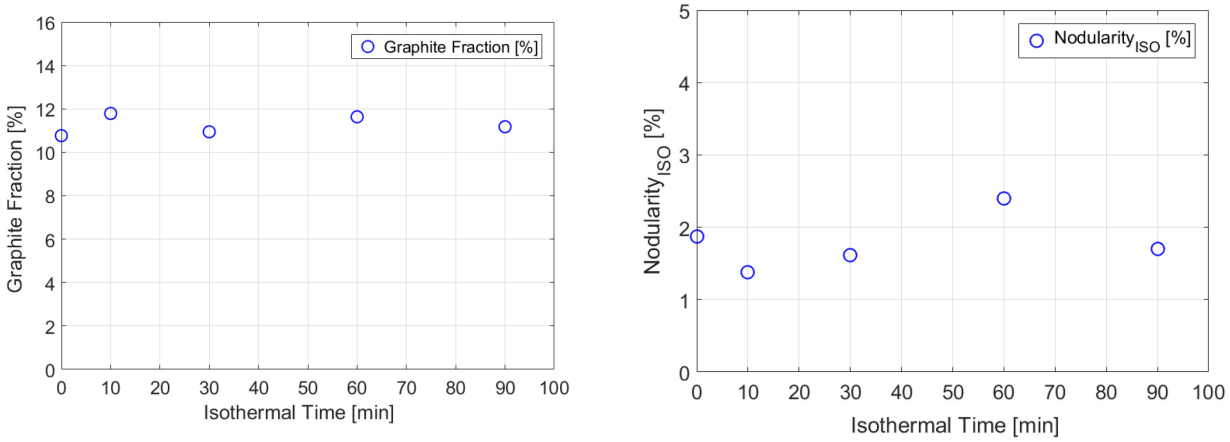

a) b)

Figure 4: a) Graphite fraction and b) nodularity values according to ISO standards measured in the samples produced in the re-started solidification series as a function of time.

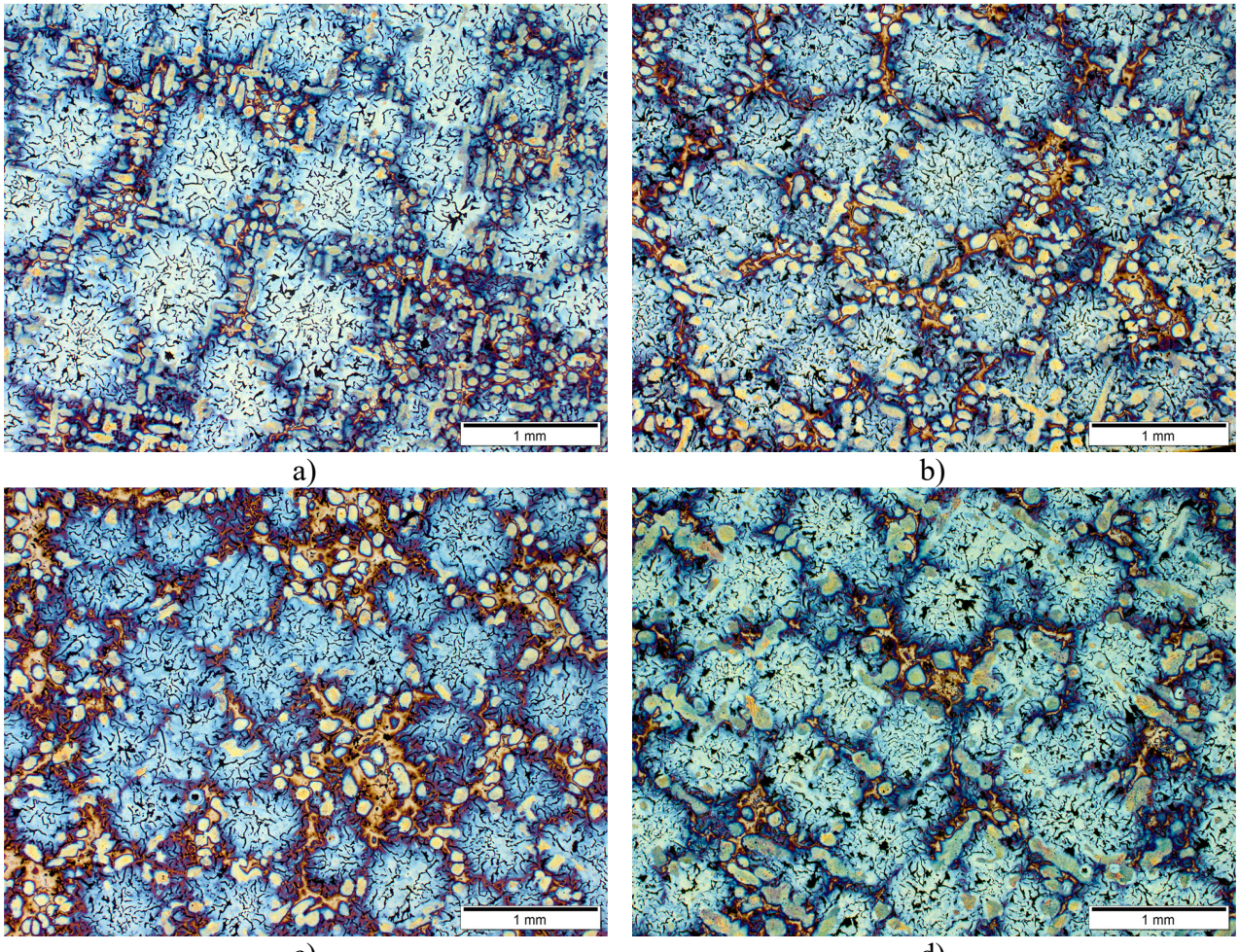

a) b)

c) d)

Figure 5: Representative colour-etched micrographs of the samples produced in the re-started solidification series after a) 0 min, b) 10 min, c) 30 min, and d) 90 min of isothermal coarsening time followed by a re-started solidification. The representative colour-etched micrograph for the sample isothermally treated for 60 min is shown in Fig. 2 b).

A preliminary qualitative observation of the colour-etched micrographs of the samples produced in the re-started solidification series, shown in Fig. 5, confirms that the morphological changes induced to the primary austenite during the primary solidification, remain present in the microstructure during the following solidification events and even after the solid-state reaction.

It can be observed in the sequence of micrographs shown in Fig. 5 how the eutectic solidification is affected by the above mentioned morphological changes in the primary austenite during the isothermal treatment. A certain influence of the coarsening time in the number, size, distribution, and morphology of the eutectic cells can be perceived. The sample coarsened for 0 min, Fig. 5 a), shows a coherent dendritic structure with a semi-ordered structure of eutectic cells "guided" by the pre-existing dendritic structure. As the isothermal coarsening time increases, the dendritic fragmentation starts, and the coherent structure begins to disappear accordingly, leading to a "less ordered" rearrangement of the eutectic cells, as can be observed in Fig 5 c) and d). A preliminary observation of the microstructural evolution shown in Fig. 5, could suggest a slight modification of the eutectic cell size, accounting, however, for a similar volume fraction occupied by eutectic cells in the micrographs.

Summary

The study of the isothermal coarsening of primary austenite in CGI has been performed combining two recently developed experimental techniques. The quantitative stereological parameters applied to the study of the coarsening process of primary austenite, M_γ, D_{IP}^{hyd}, and D_γ show a very similar behaviour to that observed in LGI in previous works, demonstrating a linear relation to $t^{1/3}$. At the same time, the coarsening rate for all the measured parameters can be considered equivalent to the one measured in LGI investigations. These two observations suggest that the coarsening process of primary austenite, occurring in the solid-liquid region during the primary solidification, is not influenced by small variations in the oxygen content between LGI and CGI melts present in the liquid that surrounds the primary dendrite network during solidification.

As it is well recognized in the literature, though, this small variation in the oxygen content does influence the shape of the graphite, giving place to the nodular, compacted and lamellar graphite morphologies. Connected to this previous knowledge, the analysis of the samples produced in the re-started solidification series shows no considerable influence of the isothermal coarsening process in the graphite fraction and nodularity. This result confirms that the fading effect of Mg can be neglected in the liquid-solid region during the primary solidification.

Further investigations are required to study the possible influence of the coarsening process of the primary austenite in the eutectic solidification using quantitative parameters related to the eutectic cells, such as size, distribution, and morphology, as can be suggested after a preliminary observation of the colour-etched micrographs captured from the samples produced in the re-started solidification series.

Acknowledgements

This research was financed by VINNOVA, the Swedish Agency for Innovation, through the research projects CastDesign, grant number (2013-03303) and SPOFIC II, grant number (2013-04720). The projects are part of a research collaboration between Scania CV AB, Volvo Powertrain Production Gjuteriet AB, Swerea SWECAST and Jönköping University. All support and contribution from these institutions are gratefully acknowledged. The authors are also grateful to Carlos Martínez-Lage and José Manuel Amieva for their technical assistance in the experiments.

References

[1] M. König, Literature review of microstructure formation in compacted graphite Iron, Int. J. Cast Met. Res. 23(3) (2010) 185-192.
[2] S. Dawson, T. Schroeder, Practical Applications for Compacted Graphite Iron, AFS Trans. 2004.
[3] D. Holmgren, Review of thermal conductivity of cast iron, Int. J. Cast Met. Res. 18(6) (2005) 331-345.
[4] V. Fourlakidis, A. Diószegi, A generic model to predict the ultimate tensile strength in pearlitic lamellar graphite iron, Mater. Sci. Eng., A 618 (2014) 161-167.
[5] L. Elmquist, A. Diószegi, Relation between SDAS and eutectic cell size in grey iron, Int. J. Cast Met. Res. 23(4) (2010) 240-245.
[6] D. Kammer, P.W. Voorhees, The morphological evolution of dendritic microstructures during coarsening, Acta Mater. 54(6) (2006) 1549-1558.
[7] P.W. Voorhees, The Theory of Ostwald Ripening, J. Stat. Phys. 38(1-2) (1985) 231-252.
[8] J.L. Fife, P.W. Voorhees, The morphological evolution of equiaxed dendritic microstructures during coarsening, Acta Mater. 57(8) (2009) 2418-2428.
[9] D.M. Stefanescu, Science and Engineering of Casting Solidification, Springer International Publishing, 2015.
[10] M.C. Flemings, T.Z. Kattamis, B.P. Bardes, Dendrite Arm Spacing in Aluminiun Alloys, in: AFS (Ed.) AFS Trans. 1991, pp. 501-506.
[11] L. Ratke, Effect of fraction solid on coarsening of secondary dendrite arms, Int. J. Cast Met. Res. 22(1-4) (2009) 268-270.
[12] M.C. Flemings, Coarsening in Solidification Processing, Mater. Trans. 46(5) (2005) 895-900.
[13] T. Cool, P.W. Voorhees, The evolution of dendrites during coarsening: Fragmentation and morphology, Acta Mater. 127 (2017) 359-367.
[14] J.C. Hernando, E. Ghassemali, A. Diószegi, The morphological evolution of primary austenite during isothermal coarsening, Mater. Charact. 131 (2017) 492-499.
[15] S.P. Marsh, M.E. Glicksman, Overview of Geometric Effects on Coarsening of Mushy Zones, Metall. Mater. Trans. A 27(3) (1996) 557-567.
[16] R. Lora, A. Diószegi, Dynamic Coarsening of 3.3C–1.9Si Gray Cast Iron, Metall. Mater. Trans. A 43(13) (2012) 5165-5172.
[17] J.C. Hernando, B. Domeij, D. González, J.M. Amieva, A. Diószegi, New Experimental Technique for Nodularity and Mg Fading Control in Compacted Graphite Iron Production on Laboratory Scale, Metall. Mater. Trans. A 48(11) (2017) 5432-5441.
[18] J.C. Hernando, A. Diószegi, An Overview of Isothermal Coarsening in Hypoeutectic Lamellar Cast Iron, Advances in the Science and Engineering of Casting Solidification, John Wiley & Sons, Inc.2015, pp. 295-302.
[19] B. Domeij, J.C. Hernando, A. Diószegi, Quantification of Dendritic Austenite After Interrupted Solidification in a Hypoeutectic Lamellar Graphite Iron, Metallogr. Microstruct. Anal. 5 (1) (2016) 28-42.
[20] ISO, ISO 16112: Compacted (vermicular) graphite cast irons — Classification, 2017.
[21] J.M. Motz, Microsegregations-An easily unnoticed influencing variable in the structural description of cast materials, Prakt. Metallogr. - PR. M. 25 (1988) 285–293.